J Mater Sci (2018) 53:11151–11166

Biomaterials

Porous poly(L-lactic acid) nanocomposite scaffolds with functionalized TiO_2 nanoparticles: properties, cytocompatibility and drug release capability

Aleksandra Buzarovska[1,*], Sorina Dinescu[2], Leona Chitoiu[2], and Marieta Costache[2]

[1] *Faculty of Technology and Metallurgy, Sts Cyril and Methodius University, Rudjer Boskovic 16, 1000 Skopje, Republic of Macedonia*
[2] *Department of Biochemistry and Molecular Biology, University of Bucharest, Spl. Independentei 91-95, 050095 Bucharest, Romania*

Received: 27 March 2018
Accepted: 5 May 2018
Published online: 14 May 2018

ABSTRACT

Cytocompatibility is one of the most important aspects in evaluating biomaterials for tissue engineering applications. In this study, biodegradable polymer scaffolds based on nanocomposites of poly(L-lactic acid) and TiO_2 nanoparticles functionalized with oleic acid (5 and 10 wt%) were prepared by thermally induced phase separation method. The aim of this research was to evaluate the properties of nanocomposite scaffolds and to investigate the influence of functionalized nanofiller on their bioactivity, biodegradability and cytocompatibility. The nanocomposite scaffolds showed bioactivity in supersaturated fluids and reduced biodegradation in simulated body fluid when compared to pure PLA scaffold. Cell viability and proliferation potential in contact with nanocomposite scaffolds were tested via MTT assay, while the scaffolds cytotoxic potential was evaluated using lactate dehydrogenase method. It was found that incorporation of functionalized TiO_2 nanofiller with content of 5 wt% in the corresponding PLA matrix has a significant positive effect on the cell viability and proliferation, while at higher nanofiller content (10 wt%), insignificant cell proliferation and increased cytotoxicity were confirmed. Furthermore, PLA/TiO_2–OA nanocomposite scaffolds were proved as promising materials for drug delivery.

Introduction

3D biodegradable polymer porous structures play a central role in tissue engineering (TE). The porous structures or scaffolds usually act as temporary templates for seeding of living cells, their growth, proliferation and regeneration of new tissues in appropriate conditions, while the biodegradable polymer matrix is subjected to biodegradation [1, 2]. Biodegradable polymer scaffolds are also widely applied as support materials for different drug loadings. Sustained and controlled release of drugs from scaffolds over a desired period of time is another important aspect in TE [3, 4].

Address correspondence to E-mail: abuzar@tmf.ukim.edu.mk; aleksbuzarovska@gmail.com

https://doi.org/10.1007/s10853-018-2415-0

In the last 15 years, a lot of materials were identified as promising for different scaffolds production. Among them, biodegradable polymers such as PLA, PCL, PGA and their copolymers have received significant scientific attention, and most of them were already approved by the FDA as materials for biomedical application [5, 6]. In spite of their recognition, some characteristics such as adequate mechanical stability, corresponding surface chemistry, controlled biodegradability and bioactivity are issues that are still open in this multidisciplinary field of research.

Some of these desired characteristics were partly accomplished by a combination of biodegradable polymers and inorganic bioactive particles [7, 8]. Nanoparticle-based composites have been the subject of intensive research due to their unique characteristics relative to other biomedical materials.

Poly(lactic acid) and its copolymers are among the most studied biodegradable polymers in this field, not only due to their relatively good mechanical properties but also because of their biodegradability into natural metabolites that have non-toxic influence on human health [9]. In recent years, the most explored PLA nanocomposites for tissue engineering were mainly based on bioactive glass ceramic nanoparticles, nanotricalcium phosphates and carbon nanotubes [10–13].

TiO_2 as nanofiller in PLA scaffolds has received considerable scientific interest [14, 15] since this ceramic filler was identified as an effective biological material due to the presence of surface OH groups that could induce formation of hydroxyapatite from simulated body fluid (SBF) [16]. In spite of the numerous published papers related to these systems, the concern related to the toxicity of nanoparticles is still an open issue. TiO_2 NPs have been shown to be toxic in several in vitro models inducing pulmonary inflammatory response [17]. However, the results related to the toxicity of these widely used nanofillers are very often controversial as a result of the existence of numerous commercial TiO_2 NPs forms (differing by size and properties). The toxicity of nanoparticles was usually correlated with their crystalline form, particle size and surface chemistry [18, 19].

Besides the toxicity, an additional problematic issue in nanocomposite scaffolds production is the agglomeration of nanoparticles within the polymer matrix that could additionally affect the nanofiller distribution and properties of nanocomposite material itself.

One of the strategies to enhance the stability of nanofillers in certain polymer matrix and to prevent their toxicity is to functionalize them properly [20]. Surface functionalization is essential for the reduction of toxicity of many NPs; therefore, it is interesting to explore how chemical or synthetic moieties on NPs interact with the living cells. In terms of cell viability, surface-modified TiO_2 NPs have been reported as materials with low cytotoxicity [21].

From this point of view, the main goal of the present study was to produce porous PLA nanocomposite scaffolds filled with oleic acid surface functionalized TiO_2 nanoparticles and to assess their influence on the bioactivity, biodegradability and cytocompatibility, as well as to evaluate their potential as drug delivery systems.

As an amphiphilic molecule belonging to the fatty acid family, oleic acid (OA) was chosen because of its non-toxicity and potential for mediation between the hydrophilic TiO_2 nanoparticles and hydrophobic PLA matrix.

Materials and methods

Materials

Poly(L-lactic acid) (M_w = 220 kDa) was obtained from Biomer, Krailling, Germany. The inorganic TiO_2 (Hombicat UV100) nanopowder was a product of Sachtleben Chemie GmbH. All solvents used in this study (dioxane, toluene, oleic acid, and ethanol) were Merck products and were used without any additional purification.

All reagents used in biological assays were purchased from Sigma-Aldrich (Steinheim, Germany) or Thermo Fisher Sci (USA). Murine preosteoblasts from MC-3T3E1 cell line were purchased from ATCC, together with the necessary culture media. Cell culture consumables were acquired from NUNC.

Surface modification of TiO_2 nanoparticles with oleic acid (OA)

The surface functionalization of TiO_2 nanoparticles with oleic acid was performed in toluene. Namely, an appropriate amount of TiO_2 was mechanically stirred in approx. 40 ml of toluene. The suspension was

additionally ultrasonically treated (Cole-Parmer 8890) for 10 min, and 7 mM of oleic acid was added to the suspension. After the suspension received slightly yellowish color, it was additionally stirred for 4 h. The resulting mixture was washed with methanol, centrifuged and vacuum-dried for 24 h.

Characterization of functionalized nanoparticles

An FTIR spectrometer (PerkinElmer Spectrum 1000) was used to confirm the attachment of the oleic acid molecules onto TiO_2 nanoparticles. The spectra were recorded in the range of 400–4000 cm^{-1} at a 4 cm^{-1} resolution, and 64 scans were averaged. The FTIR spectra of unmodified and modified TiO_2 nanoparticles were obtained using attenuated total reflection (ATR) method.

Thermogravimetric analysis of unmodified and functionalized nanoparticles was performed on a PerkinElmer, Pyris Diamond analyzer in a temperature range between 30 and 700 °C, at a heating rate of 10° min^{-1}, under constant nitrogen flow (50 cm^3 min^{-1}).

Preparation of PLA nanocomposite scaffolds

The PLA/TiO_2–OA nanocomposite scaffolds were prepared using thermally induced phase separation (TIPS) method, by applying freeze-extraction method using ethanol in order to remove the frozen solvent. PLA was dissolved in dioxane for 2 days in order to obtain a stable solution. A given amount of OA modified nanoparticles (5 and 10 wt% related to the polymer) was suspended in dioxane and ultrasonically treated for 60 min. The polymer solution and TiO_2-dioxane suspension were mixed together to produce 5% (w/v) PLA-dioxane solution. The obtained mixture was ultrasonically treated for 30 min and then frozen at − 30 °C. The solvent extraction was performed with pre-cooled ethanol. The extracting solvent was changed every 24 h during 72 h. The solvent extracted samples were vacuum-dried at room temperature. For comparison purposes, PLA scaffolds filled with unmodified TiO_2 (5 and 10 wt%) nanoparticles were also prepared. The designations of prepared scaffolds are given in Table 1.

Table 1 Composition and designation of PLA scaffolds

Sample	PLA (wt%)	TiO_2–OA (wt%)	TiO_2 (wt%)
PLA	100	0	0
PLA/TiO_2–OA-5	95	5	0
PLA/TiO_2–OA-10	90	10	0
PLA/TiO_2-5[a]	95	0	5
PLA/TiO_2-10[a]	90	0	10

[a]Polymer scaffolds prepared for some comparisons

Characterization of PLA/TiO_2–OA nanocomposite scaffolds

The prepared PLA/TiO_2–OA nanocomposite scaffolds were analyzed by FTIR spectroscopy for the wavelength range of 400–4000 cm^{-1}, using the same instrument as described above. FTIR spectroscopy was used to determine the influence of the functionalized nanofiller on the crystalline sensitive bands and to determine the crystalline indices.

The glass transition, melting temperature and degree of crystallinity were determined by differential scanning calorimetry, using TA Instruments DSC-Q-200. The samples were heated from − 20 °C up to 220 °C at a heating rate of 10 °C min^{-1}. The degree of crystallinity was determined as a ratio between the enthalpy of fusion ΔH_f and the ΔH_f^0 taken as 93.2 kJ mol^{-1} [22].

The apparent density (ρ) was obtained by measuring the mass (m) and the volume (v) of the scaffold, while the porosity was determined as [23]:

$$\varepsilon = 1 - \rho/\rho_p \quad (1)$$

where ρ_p is the bulk density of the scaffold composite.

The pore structure and morphology of the prepared samples were studied with a scanning electron microscope (Philips 515) with accelerating voltage of 15 kV. The observed specimens were taken from the inner part of the scaffolds and metallized with gold.

The compressive modulus were measured on cylindrical samples (n = 5) (with ~ 20 mm diameter and ~ 5 mm height), at a static load of 5 kg and cross-head speed of 1 mm min^{-1}, using TA.XT Stable Micro System, UK.

Hydrolytic biodegradation

The hydrolytic biodegradation was followed in a simulated body fluid (SBF), prepared according to the Kokubo procedure [24] and buffered at adjusted pH = 7.4 using HCl (Merck). The scaffolds were placed in vials containing 15 ml of the SBF solutions at constant temperature of 37 °C. The degradation was observed for a period of 7, 14, and 28 days by using FTIR spectroscopy and analyzing the characteristic peaks of PLA.

In vitro bioactivity

The potential bioactivity of the PLA–TiO_2–OA scaffolds was tested in supersaturated fluids prepared according to [25]. The investigated scaffolds were immersed in Ca/P supersaturated fluid for 6 h and characterized by SEM.

Water uptake measurements

The water uptake behavior of the prepared scaffolds was studied in phosphate buffer solution (PBS), (pH = 7.4) at 37 °C. The precisely weighed scaffolds were measured before and after immersion in PBS after a certain period of time (4, 8, 24, 48 and 96 h). The wetted scaffolds were wiped with soft paper before each measurement. The degree of water uptake at the time t was calculated using equation:

$$WU = (W_t - W_o)/W_o \cdot 100 \quad (2)$$

where W_o is the weight of dry scaffold and W_t is the weight of wet scaffold after relevant time periods t.

Drug loading and release

Salicylic acid with high purity (Merck product) was used as a model drug in our investigations. The experiments were carried out by immersing the weighed scaffolds (0.05 g) in model drug solution in ethanol with initial concentration of 0.01 g ml^{-1}. After mildly stirring for 48 h at room temperature, the scaffolds were gently removed from the model drug solution. The relative amount DL of loaded model drug in each scaffold was calculated from the equation:

$$DL = V(C_0 - C_l)/w \quad (3)$$

where V is the volume of model drug solution in (ml), C_o is the initial concentration of salicylic acid in ethanol, C_1 is the concentration of model drug solution after loading process, and w is weight of the scaffold (g).

Each loaded scaffold was immersed in 10 ml of phosphate buffered saline (pH = 7.4) at 37 °C applying mild stirring. The in vitro release profile of the model drug was followed by UV/VIS spectrometer (HP 8452) at 296 nm. The calibration curve was obtained with the model drug in concentration range of 0.2–15 μg ml^{-1}, where the curve was linear, following the Beer's law.

Cell viability and proliferation potential

Murine preosteoblasts from MC-3T3E1 cell line were cultivated in direct contact with PLA/TiO_2 and PLA/TiO_2–OA nanocomposite scaffolds. Cell suspension was allowed to distribute in the volume of the scaffolds, resulting in 3D cell-scaffold cultures, which were maintained in standard culture conditions (37 °C, 5% CO_2 and adequate humidity) for up to 7 days.

Cell viability and proliferation potential in contact with nanocomposite scaffolds were tested via MTT assay, after 2 and 7 days of culture. Briefly, the cell-scaffold constructs were incubated with 1 mg/ml MTT solution for 4 h at 37 °C and the resulted formazan crystals were solubilized afterward with isopropanol. The optic density of the resulting solution was measured by spectrophotometry at 550 nm.

PLA/TiO_2–OA nanocomposite scaffolds cytotoxic potential was tested using lactate dehydrogenase (LDH) method and compared to the cytotoxic potential of PLA/TiO_2 nanocomposite scaffolds. The culture media was briefly collected from the 3D cultures and mixed with the components of the kit (Tox7-KT, Sigma, Steinheim, Germany), according to manufacturer's instructions. The resulting solution was measured by spectrophotometry at 490 nm on Flex Station 3 (Molecular Devices, USA).

LiveDead assay was used as a qualitative method to highlight the ratio between live (green cells) and dead (red cells) using calcein-AM and ethidium bromide homodimer (EthD-1) fluorescent dyes. After 30 min of incubation with the mixed solution, images were obtained in confocal microscopy using Zeiss LSM 710 system and corresponding ZEN software.

In order to investigate cell adhesion to the biomaterials, F-actin filaments were stained using a phalloidin-FITC solution. Cells were fixed with 4%

paraformaldehyde (PFA) for 1 h at 4C and then permeabilized with a solution containing 1% Triton-X100. Cytoskeleton filaments staining were performed for 1 h in dark conditions, followed by nuclei staining with DAPI and visualization in confocal microscopy.

All tests were performed in triplicate. Statistical analysis of the data was carried out using Graph Pad Prism software, considering a p value < 0.05 to be statistically significant.

Results and discussion

Characterization of surface-modified TiO_2 nanoparticles

FTIR spectroscopy was used to verify the proper surface functionalization of TiO_2 nanoparticles with oleic acid (OA). The FTIR spectra of TiO_2 and TiO_2–OA NPs are shown in Fig. 1. FTIR spectrum of uncoated TiO_2 NPs showed intensive extended band at 3400 cm^{-1} as well as small intensity band at 1630 cm^{-1} due to the stretching and bending vibrations of hydroxyl groups on the surface of TiO_2 nanoparticles [26]. In FTIR spectrum of modified TiO_2 (TiO_2–OA), the intensity of the peak that appeared between 3000 and 3700 cm^{-1}, decreased showing suppression of OH vibration mode that could be considered as an evidence for lower content of surface OH groups. Additionally, new absorption bands positioned at around 2800–3000, 1460, 1519 and 1433 cm^{-1} could be observed. The bands located at 2924 and 2854 cm^{-1} were ascribed to the asymmetric and symmetric stretch vibrations of CH_2 groups of oleic acid, while the very small in intensity band around 1460 cm^{-1} was due to the deformation bending mode of CH_2 groups [26]. The peaks positioned at 1519 and 1433 cm^{-1} were ascribed to $\nu(COO)_{asym}$ and $\nu(COO)_{sym}$ vibrations, respectively [26]. The difference between these two vibrations $\Delta\nu_{a-s}$ of 86 $cm^{-1} < 110$ corresponds to the literature value, which is characteristic for bidentate chelating coordination between Ti atoms and carboxylic groups of oleic acid [27]. The appearance of characteristic bands of oleic acid confirmed the successful functionalization of TiO_2 NPs.

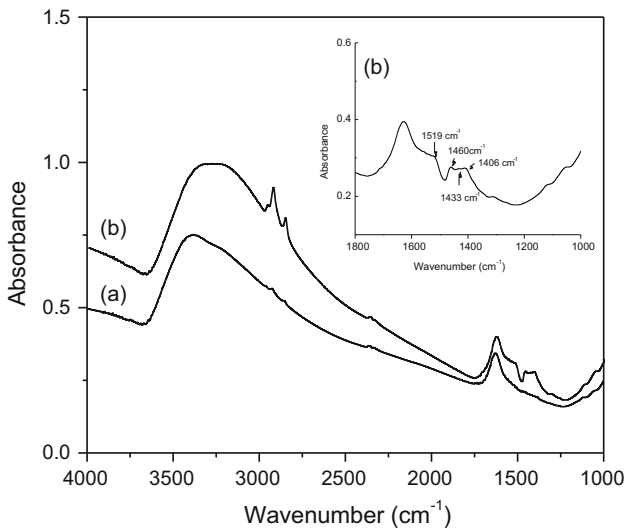

Figure 1 FTIR spectra of bare TiO_2 (a) and functionalized TiO_2 nanoparticles with oleic acid (b).

The degree of surface functionalization was determined by TG analysis. Figure 2a shows thermogravimetric curves of TiO_2 unmodified nanoparticles and TiO_2–OA NPs. The weight loss of TiO_2 NPs up to 200 °C (7.61%) was due to the physically absorbed water, while the weight loss between 200 and 400 °C (5.65%) was associated with the removal of surface OH groups. In the TGA curve of TiO_2–OA NPs, after gradual loss of water molecules (4.78%), the weight loss of about 2.69% up to 320 °C might be due to the loss of OH surface groups and removal of free oleic acid. Further degradation beyond 320 °C corresponded to decomposition of bonded oleic acid to TiO_2 NPs (5.76%). Typically, ligands that are bonded more strongly to the nanoparticles decompose at higher temperatures [28], as it is shown in Fig. 2a. The last weight loss of 5.76% could actually confirm that almost all surface OH groups are theoretically functionalized with OA. The above considerations were verified by analyzing the DTG data. The DTG curves related to unmodified TiO_2, modified TiO_2–OA NPs, and oleic acid are shown in Fig. 2b. The DTG curve of TiO_2 NPs exhibited a DTG peak positioned at 78.1 °C, while the DTG curve for TiO_2–OA showed two DTG peaks (positioned at 87.7 and 422 °C) and a small shoulder at 353 °C. The free unbonded oleic acid showed DTG peak at about 314 °C, thus confirming the above TGA results.

Taking into account the results obtained from FTIR spectroscopy and thermogravimetric measurements, it could be concluded that proper functionalization of nanoparticles was achieved.

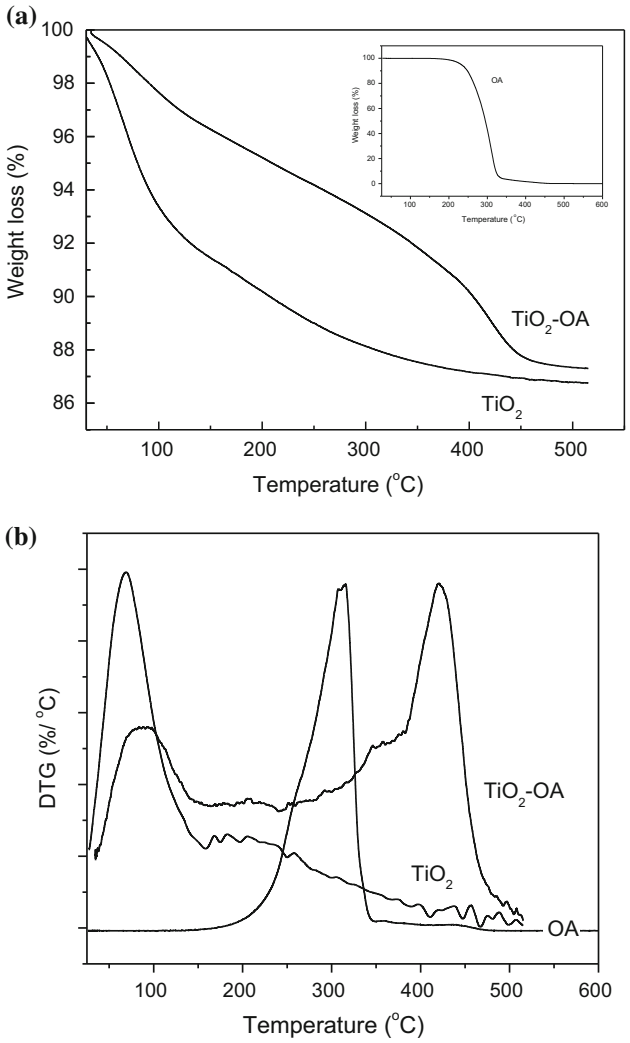

Figure 2 **a** TGA curves of oleic acid, bare and functionalized TiO_2 NPs. **b** DTG curves of oleic acid, bare and functionalized TiO_2 NPs.

Characterization of PLA/TiO_2–OA nanocomposite scaffolds

FTIR characterization was performed in order to analyze the influence of modified nanofiller on the molecular structure of PLA.

FTIR spectra of the investigated samples are presented in Fig. 3. Characteristic peaks of pure PLA scaffold at 1754, 1454, 1383 and 1181 cm^{-1} were assigned to C=O stretching vibration, CH_3 asymmetric and symmetric deformations and C–O–C stretching vibrations, respectively [29]. The shoulder absorption band positioned at 1210 cm^{-1} was ascribed to C–O–C stretching vibrations characteristic for crystalline phase. It could be noted that the

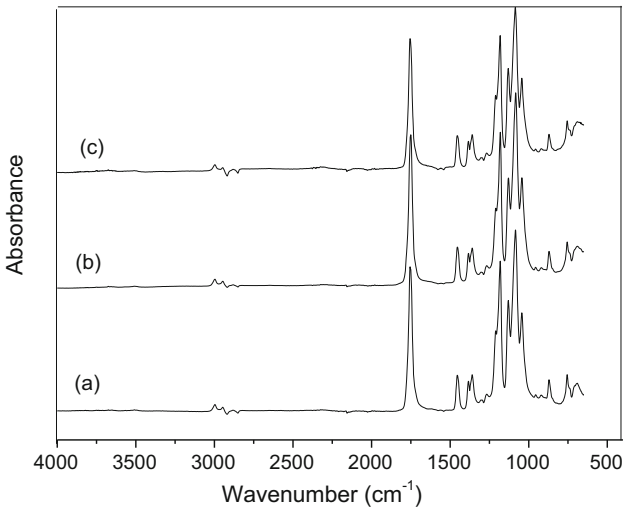

Figure 3 FTIR spectra of PLA (a), PLA/TiO_2–OA-5 (b), and PLA/TiO_2–OA-10 (c) nanocomposite scaffolds.

incorporation of functionalized TiO_2 nanoparticles in the corresponding PLA matrix had no pronounced influence on the absorption peaks characteristic for PLA matrix, but certain influence on crystallinity indices was identified. Namely, the crystallinity index for each scaffold was determined as the ratio of the intensities of the bands positioned at 1180 and 1382 cm^{-1} [30] and was as follows: 6.6, 7.4 and 7.6 for the PLA, PLA–TiO_2–OA-5, and PLA–TiO_2–OA-10, respectively.

The increased crystallinity indices determined in the nanocomposites confirmed the increased crystallinity of polymer matrix with the increase in TiO_2–OA nanofiller content. Similar results were previously reported, showing improved crystallinity in PLA composites filled with TiO_2 nanoparticles [31].

The first DSC runs at a heating rate of 10° min^{-1} were analyzed in order to comment the actual crystallinity developed during the preparation procedure of all investigated scaffolds. All relevant data are

Table 2 Thermal properties of PLA/TiO_2 and PLA/TiO_2–OA nanocomposite scaffolds

Scaffold	T_g (°C)	T_m (°C)	ΔH_f (J g^{-1})	X_c (%)
PLA	67	168.8	40.1	43.0
PLA/TiO_2–OA-5	68	169.1	40.6	45.8
PLA/TiO_2–OA-10	67	169.0	42.1	50.2
PLA/TiO_2-5[a]	67	169.2	40.3	45.5
PLA/TiO_2-10[a]	68	169.0	40.0	47.6

[a]Control measurements

collected in Table 2. It could be noted that the glass transition temperature in PLA and its composite scaffolds was around 67 ± 1 °C. This insignificant change in glass transition temperature supports the conclusion that nanofiller particles did not affect the mobility of PLA chains. The melting peak temperature of PLA was located around 169 ± 1 °C in both polymer nanocomposite scaffolds. The normalized degree of crystallinities (Table 2) showed higher X_c values with the increase in functionalized TiO_2 nanopaticles when compared to the X_c value relevant for pure PLA scaffold. Similar results were obtained in PLA nanocomposite scaffolds filled with TiO_2 unmodified nanoparticles [32].

The increased degrees of crystallinity confirmed by DSC data correspond very well with the increased crystallinity indices obtained by FTIR analysis. This additionally supports the hypothesis that such a behavior might be due to the nucleation ability of nanoparticles, as reported in the literature [33].

The pore quality and pore size in polymer scaffolds, prepared by thermally induced phase separation method, could be generally controlled by the initial polymer concentration and cooling rate of polymer solution during the preparation procedure [34]. The polymer concentration of 5% (w/v) and slow cooling process were taken as an optimal condition for production of polymer scaffolds with highly porous structures, based on previously published results [32].

Both densities and porosities of PLA/TiO_2–OA nanocomposite scaffolds are listed in Table 3 and compared to those relevant to PLA/TiO_2 nanocomposite scaffolds.

The measured porosities of the investigated scaffolds (determined according to Eq. 1) were around 92%. It could be noted that the nanofiller has no noticeable influence on the apparent densities at nanofiller content of 5 wt%, while at 10 wt% content of TiO_2–OA a slightly increased density could be observed. Similar results were obtained for the control group of nanocomposite scaffolds prepared with unmodified TiO_2 NPs.

Table 3 Densities and porosities of PLA nanocomposite scaffolds

Sample	Density (g cm^{-3})	Porosity (%)
PLA	0.092 ± 0.007	92 ± 0.56
PLA/TiO_2–OA-5	0.094 ± 0.005	92 ± 0.40
PLA/TiO_2–OA-10	0.103 ± 0.004	91 ± 0.30
PLA/TiO_2-5	0.090 ± 0.006	92 ± 0.51
PLA/TiO_2-10	0.108 ± 0.005	91 ± 0.47

Measurements averaged of $n = 3$

SEM microscopy was used to analyze the morphology of the prepared scaffolds and to evaluate the dispersibility of the added nanofiller. SEM images of PLA nanocomposite scaffolds are shown in Fig. 4. A highly porous, anisotropic architecture could be seen in all investigated composite scaffolds, with characteristically interconnected and elongated pores with lengths ranged between 70 and 150 μm and wall thickness between 7 and 12 μm. Similar morphologies were obtained in PLA/TiO_2 nanocomposite scaffolds prepared by the same method [32]. Nanofiller content of 5 and 10 wt% seems to have no significant influence on the pore architecture, as was also confirmed by the porosity measurements. In the filled composite scaffolds, nice and evenly distributed nanoparticles were observed as small white dots (Fig. 4). Certain agglomerates with dimensions lower than 0.5 μm were identified, especially in the nanocomposite scaffold with 10 wt% of the nanofiller. Additionally, these small agglomerates were evenly dispersed, acting as larger particles within the polymer matrix. Morphologically it could be concluded that the nanofiller was well distributed, but comparing to the previously published results [32], the functionalization of TiO_2 nanoparticles with oleic acid did not significantly affect their dispersibility. The reason for such a behavior could be ascribed to the restricted diffusion process of TiO_2–OA NPs within the viscous polymer solution, which has an additional influence on the distribution process.

The addition of nanofillers was expected to improve the mechanical properties of the prepared scaffolds, and it is usually correlated with the improved nanofiller dispersibility.

The compressive strength was not measured in this study, because all investigated scaffolds were compressed under applied load without fracture. The compressive modulus were determined from the linear part of the stress–strain curves as 2.79, 2.91 and 2.10 MPa for the PLA, PLA/TiO_2–OA-5 and PLA/TiO_2–OA-10, respectively. Only a slight increase in the compressive modulus was detected in PLA/TiO_2–OA-5 nanocomposite, while the compressive modulus in PLA/TiO_2–OA-10 nanocomposite had a decreased value. Polymer scaffolds with high

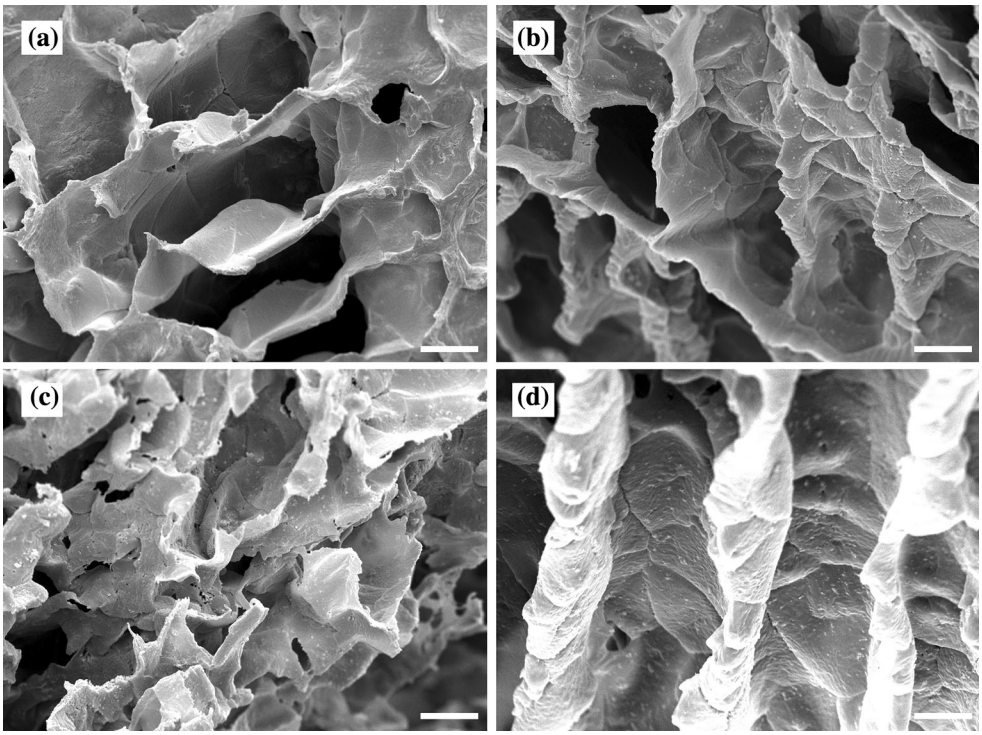

Figure 4 SEM images of the morphology of PLA (**a**), PLA/TiO_2–OA-5 (**b**), PLA/TiO_2–OA-10 (**c**) and PLA/TiO_2–OA-10 (**d**) nanocomposite scaffolds. Scale bars: a, b, c = 20 μm; d = 10 μm.

porosity (above 80%) have moduli of approximately 0.5–5 MPa, depending on the material and scaffold density [35, 36].

Bioactivity evaluation

The bioactivity evaluation is usually connected to the process of formation of hydroxyapatite layers when treating the samples in biological fluids. The properties of the hydroxyapatite layer, which is an important component in bone tissue engineering, can additionally affect the cell viability and proliferation [37]. The method used in this study for evaluating the bioactivity of scaffolds is fast and simplified, instead of the slow methods of scaffolds treatment in simulated body fluid (SBF) that sometimes need very long times (more than 15 days) to evaluate their bioactivity. The SEM micrographs, obtained after scaffolds treatment for 6 h in calcifying solutions, are presented in Fig. 5. It is obvious that 6 h of treatment of pure PLA scaffold induce formation of hydroxyapatite clusters that appear only at certain areas on the scaffold surface, and certain colonies of HA could be observed but with lower dimensions when compared to HA induced onto nanocomposite scaffolds. These clusters were more pronounced in nanocomposite scaffolds. Moreover, the 6 h treatment time of polymer scaffolds was long enough to identify hydroxyapatite cores, present not only on the surfaces of the scaffolds but also deeper in the inner sections of the scaffold pores. From the presented images, it seems that scaffolds filled with TiO_2 modified particles also induce enhanced formation of hydroxyapatite, despite the fact that the reactive surface of TiO_2 nanoparticles (OH groups) was replaced with long oleic acid tails.

Determination of water uptake

The water uptake behavior usually describes the ability of scaffolds to preserve water and is an important parameter in tissue engineering and drug delivery systems. In TE applications, the material should possess certain hydrophilicity, since insufficient water absorption inhibits cell growth [38]. As the functionalization of TiO_2 nanoparticles induced lower content of surface OH groups, it was interesting to follow the water uptake behavior of the composites prepared with OA modified nanoparticles. The effect of filler loading on the water uptake of

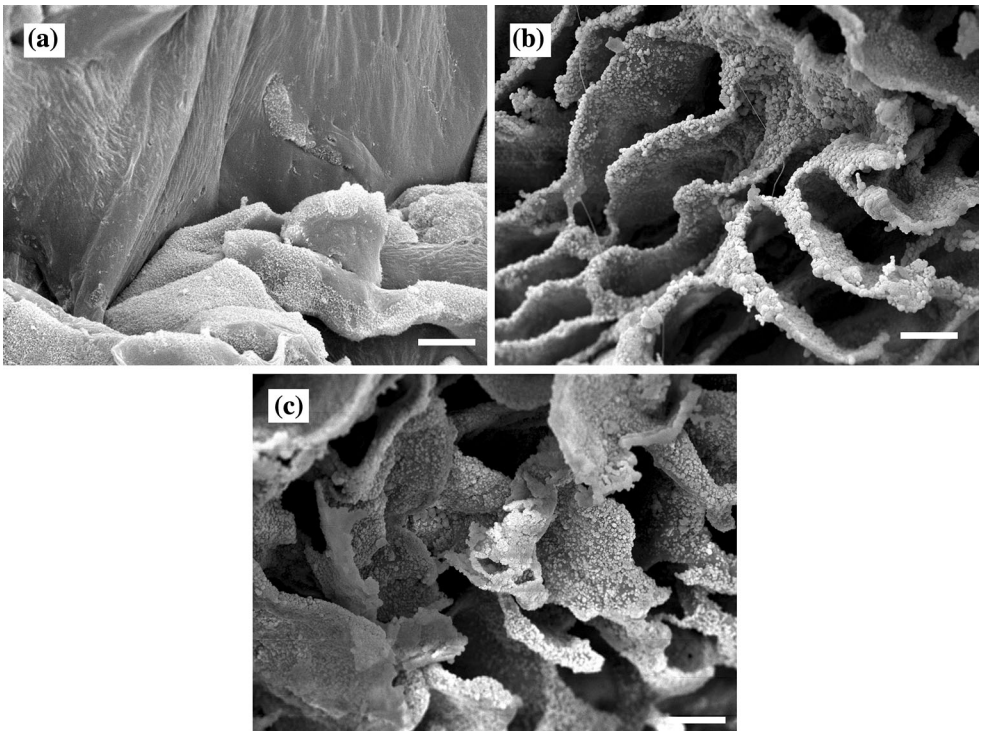

Figure 5 SEM images of PLA (**a**), PLA/TiO_2–OA-5 (**b**), and PLA/TiO_2–OA-10 (**c**) nanocomposite scaffolds treated in supersaturated fluids for 6 h. Scale bars: a = 5 μm; b, c = 20 μm.

nanocomposite scaffolds as a function of time is presented in Fig. 6. It could be observed that water uptake increased with the increase in soaking time in PBS. It could be seen that nanocomposites filled with TiO_2–OA NPs have lower water uptake capability when compared to the water uptake behavior of neat PLA scaffold and PLA scaffolds filled with unmodified TiO_2 nanoparticles, given here for comparison. It was also evident that the two nanocomposites (PLA/TiO_2–OA-5 and PLA/TiO_2–OA-10) have almost similar trends in water uptake behavior, thus confirming that there was no influence of the nanofiller content.

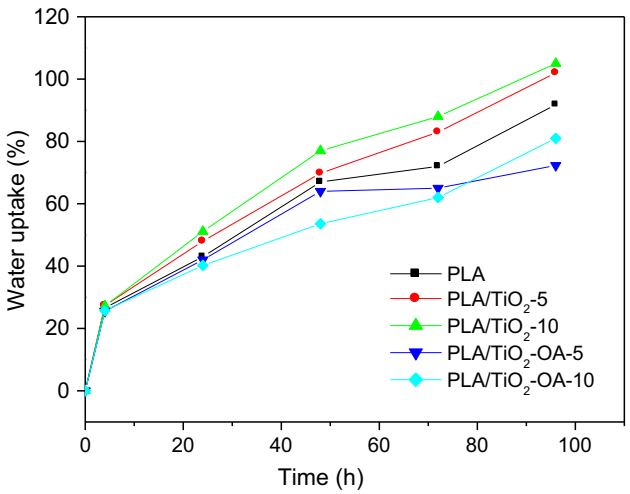

Figure 6 Water uptake behavior in PLA/TiO_2–OA and PLA/TiO_2 nanocomposite scaffolds.

In PLA scaffolds with porosity lower than 80%, the water uptake was about 25%, mainly due to the capillary action of the material [39]. For a prolonged immersion time, water absorption of about 150% was reported by Guo et al. [40].

Biodegradability of the PLA/TiO_2–OA scaffolds

Hydrolytic degradation is an important aspect in designing materials for biomedical applications. The biodegradation was carried out in SBF solution at 37 °C for the duration of 7, 14 and 28 days, and the treated samples were subjected to FTIR analysis. The summary FTIR spectra of untreated and treated scaffolds (PLA and PLA/TiO_2–OA-5) in SBF are presented in Fig. 7a and b. It is obvious that except the peak intensity changes of certain characteristic bands of PLA, no significant changes could be

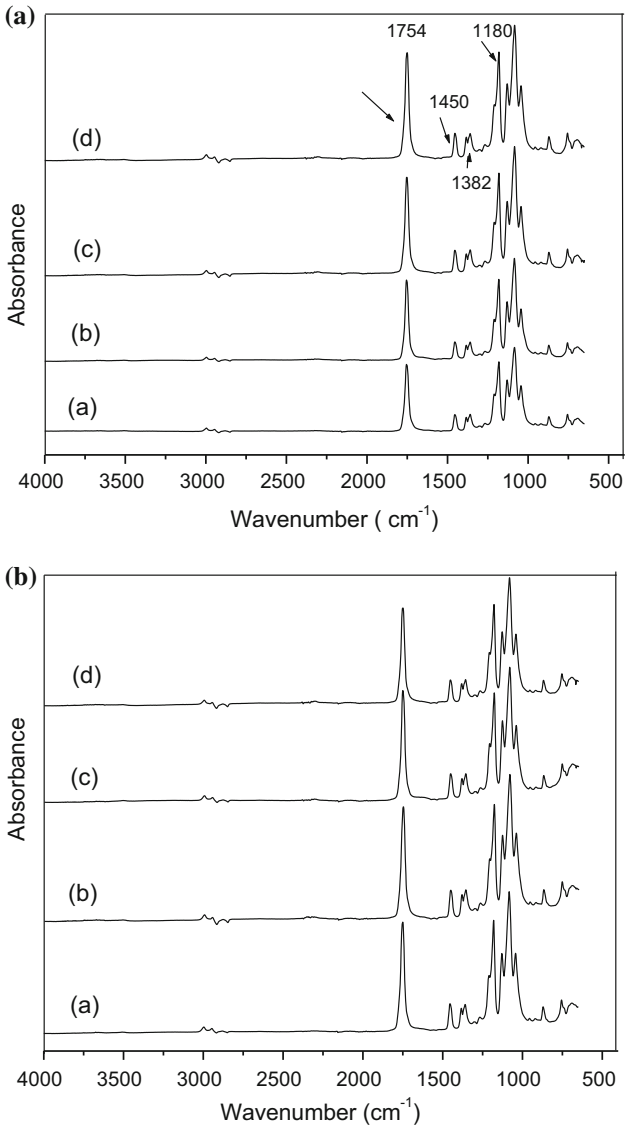

Fig. 7 **a** FTIR spectra of PLA scaffolds immersed in SBF for 0 days (a), 7 days (b), 14 days (c) and 28 days (d). **b** FTIR spectra of PLA/TiO_2–OA-5 nanocomposites incubated in SBF for 0 days (a), 7 days (b), 14 days (c), and 28 days (d).

identified. Accordingly, the crystallinity as well as carbonyl indices were determined as a function of time (Table 4). The crystallinity index for PLA scaffold treated in SBF tends to increase, while in PLA/TiO_2–OA-5 and PLA/TiO_2–OA-10 scaffolds the CI's were almost constant. During the degradation, the process primarily occurs on the amorphous parts of the sample, thus increasing the total crystallinity of the system [41]. This behavior clearly confirms that the biodegradation during the investigated period of time proceeded in pure PLA scaffold, while in scaffolds filled with TiO_2–OA the biodegradation was considerably restricted. The restricted biodegradation in filled composites was supported by the estimated carbonyl indices, determined as the ratio of the peak intensities corresponding to carbonyl stretching at 1754 cm^{-1} and CH_2 bending at 1450 cm^{-1} [42]. Namely, the carbonyl indices of PLA scaffolds as a function of time decreased continuously, while for PLA/TiO_2–OA-5 and PLA/TiO_2–OA-10 composites, these values are almost constant, thus confirming the fact that the biodegradation within the investigated period of up to 28 days was considerably limited. Contrary to this, the literature data related to PLA systems filled with TiO_2 nanoparticles showed that the biodegradation was considerably improved when compared to unfilled PLA matrix, supporting the hypothesis that biodegradation is drastically influenced by the reactive surface OH groups [43].

Drug loadings and release

The ability of polymer scaffolds to serve as controlled drug releasing systems is a very important aspect in tissue engineering, since these template materials are capable of releasing certain drug over a desired period of time. The drug loading and release primarily depend on physicochemical properties of the

Table 4 Crystallinity and carbonyl indices of PLA and its nanocomposites after immersion in SBF

Period of immersion in SBF	CI (I_{1180}/I_{1382})			Carbonyl index (I_{1754}/I_{1450})		
	PLA	PLA–TiO_2–OA-5	PLA–TiO_2–OA-10	PLA	PLA–TiO_2–OA-5	PLA–TiO_2–OA-10
0	6.6	7.4	7.6	4.7	4.5	4.6
7	7.1	7.3	7.3	4.1	4.4	4.7
14	7.2	7.4	7.3	3.9	4.4	4.7
28	8.3	7.5	7.4	3.7	4.5	4.8

polymer scaffold, its porosity and biodegradability [44, 45].

The contents of the loaded model drug in all investigated scaffolds are given in Table 5. For comparison, the results of PLA composites with TiO_2 unmodified nanoparticles are also presented. It could be seen that the loading efficiencies were almost constant in all investigated composites. The surface OH groups of unmodified TiO_2 nanoparticles should attract the model drug more easily, since salicylic acid also possesses functional OH groups [46, 47]. However, since the model drug loadings were performed in ethanol, medium that actually increased the hydrophilicity of all systems, regardless if the scaffolds were filled with unmodified TiO_2 or TiO_2–OA nanoparticles, the loading concentrations were almost similar.

The releasing profiles for all samples are presented in Fig. 8. It could be seen that the release process was intensive in the first 4 h, while during prolonged periods of time this process was slowed down. Such a behavior could be explained by the fact that usually during the first 5 h, surface absorbed drug is released (fast releasing), while the drug absorbed within the scaffold structure is released by diffusion controlled mechanism (slow releasing process) [48]. As it is presented, the amount of drug release increased in PLA/TiO_2 nanocomposites, while in PLA/TiO_2–OA scaffolds the drug release was decreased. These results are in close correlation with the water uptake measurements given in Fig. 6. Namely, the systems that exhibited improved water uptake facilitate the diffusion process, causing improved diffusion of the model drug. The water absorption in PLA/TiO_2–OA systems was lower; the diffusion of the model drug was suppressed, causing slower drug releasing [49]. Within 24 h, between 20 and 24% of the absorbed drug was released. In spite of the fact that these releasing profiles do not differ from each other dramatically, nevertheless by proper NPs functionalization and proper content of added nanofiller, the controlled drug release could be additionally tailored, giving these systems a promising potential for targeted drug delivery.

Table 5 Drug loadings within PLA nanocomposite scaffolds

Scaffold type	Drug loading mg/0.05 g scaffold
PLA	7.82
PLA/TiO_2–OA-5	7.78
PLA/TiO_2–OA-10	7.59
PLA/TiO_2-5	7.74
PLA/TiO_2-10	7.76

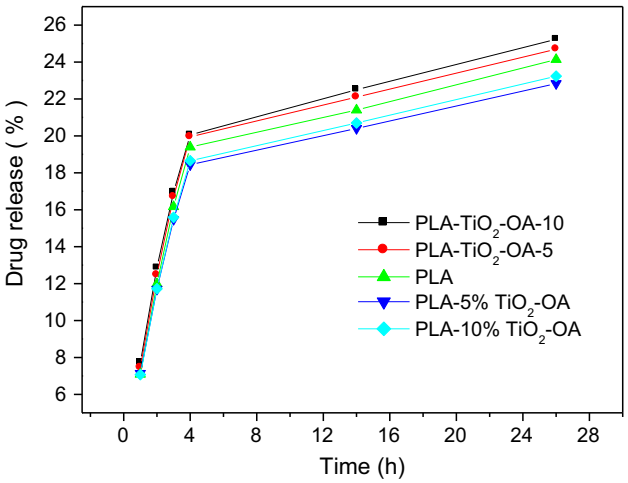

Figure 8 Drug-releasing profiles for PLA/TiO_2 and PLA/TiO_2–OA nanocomposite scaffolds.

Cell viability and proliferation potential in contact with PLA/TiO_2 composites

PLA/TiO_2–OA and PLA/TiO_2 nanocomposites were comparatively tested for the ability to support pre-osteoblasts growth and development in the context of possible bone tissue regeneration.

Cell viability in contact with the investigated materials was quantitatively evaluated by MTT assay, and important differences between the composites were revealed during 1 week of analysis (Fig. 9). Based on MTT assay results, the cells displayed similar profile of cell viability 3 days after cell seeding in contact with the scaffolds. The only statistically significant difference in viability ($p < 0.01$) was reported for PLA/TiO_2–OA-5, as compared to the PLA control scaffold. After 1 week of culture in standard conditions, a higher proportion of viable cells was found in contact with PLA/TiO_2-10 ($p < 0.001$) and PLA/TiO_2–OA-5 ($p < 0.001$) than in contact with pure PLA control sample. Interestingly, similar levels of cell viability were quantified for PLA/TiO_2–OA-10 and PLA control scaffold. This finding may suggest that the addition of TiO_2 nanofiller in the PLA matrix and its functionalization with oleic acid has a positive impact on cell behavior and growth, but the addition of nanoparticles in excess (10 wt%) appears to inhibit cell viability.

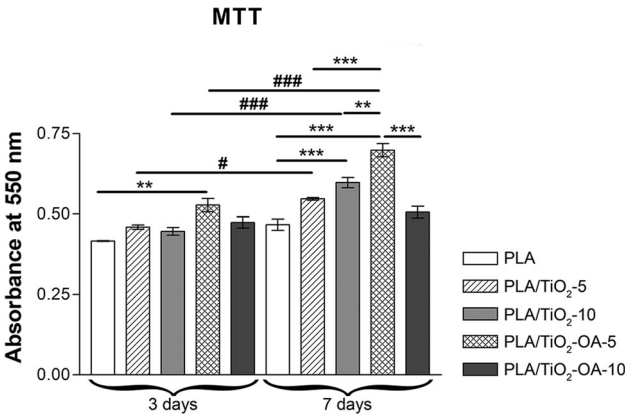

Figure 9 Cell viability and proliferation in contact with PLA/TiO_2 materials as revealed by MTT test after 7 days of standard culture. Statistical significance: $**p < 0.01$ [PLA/TiO_2–OA-5 3 days vs. PLA 3 days; PLA/TiO_2–OA-5 7 days vs. PLA/TiO_2-10 7 days]; $***p < 0.001$ [PLA/TiO_2-10 7 days vs. PLA 7 days; PLA/TiO_2–OA-5 7 days vs. PLA 7 days; PLA/TiO_2–OA-10 7 days vs. PLA/TiO_2–OA-5 7 days; PLA/TiO_2–OA-5 7 days vs. PLA/TiO_2-5 7 days]; # $p < 0.05$ [PLA/TiO_2-5 7 days vs. PLA/TiO_2-5 3 days]; ### $p < 0.001$ [PLA/TiO_2-10 7 days vs. PLA/TiO_2-10 3 days; PLA/TiO_2–OA-5 7 days vs. PLA/TiO_2–OA-5 3 days].

In terms of proliferation, no significant proliferation was registered for PLA scaffold between 3 and 7 days of culture. Similar profile was also observed for PLA/TiO_2–OA-10 sample. In contrast, cells cultivated in contact with PLA/TiO_2-5 registered a slight proliferation ($p < 0.05$) from 3 to 7 days of culture, whereas highest proliferation rates were reported for PLA/TiO_2-10 and PLA/TiO_2–OA-5 composites, confirming the first conclusions of the viability tests. Therefore, the most biocompatible composites in terms of cell viability and proliferation appear to be PLA/TiO_2-10 and PLA/TiO_2–OA-5, as compared to the pure PLA control sample.

Cytotoxic potential of PLA/TiO_2 composites

The proportion of dead cells in the 3D cultures, shown by the levels of released LDH in the culture media, was informative for the cytotoxic potential of PLA/TiO_2–OA nanocomposites comparing with PLA/TiO_2 nanocomposite scaffolds (Fig. 10). Similar levels of basic cytotoxicity were displayed by PLA–TiO_2-5, PLA–TiO_2-10 and PLA–TiO_2–OA-5 nanomaterials after 3 days of culture, related to PLA control sample, whereas a statistically significant increased cytotoxicity was registered for PLA–TiO_2–OA-10

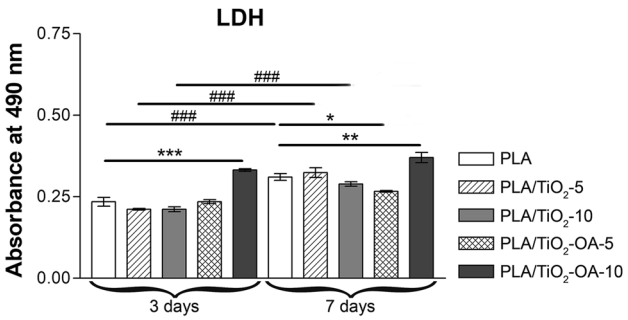

Figure 10 PLA/TiO_2 materials cytotoxicity over 7 days of culture as shown by LDH assay. Statistical significance: $*p < 0.05$ [PLA/TiO_2–OA-5 7 days vs. PLA 7 days]; $**p < 0.01$ [PLA/TiO_2–OA-10 7 days vs. PLA 7 days]; $***p < 0.001$ [PLA/TiO_2–OA-10 3 days vs. PLA 3 days]; ### $p < 0.001$ [PLA 7 days vs. PLA 3 days; PLA/TiO_2-5 7 days vs. PLA/TiO_2-5 3 days; PLA/TiO_2-10 7 days vs. PLA/TiO_2-10 3 days].

composite ($p < 0.001$). After 7 days of culture, this difference was maintained, but to a lower degree ($p < 0.01$). Interestingly, the cytotoxic potential of PLA/TiO_2–OA-5 was found to be lower than the one of the control PLA sample ($p < 0.05$), supporting the data obtained for cell viability and proliferation.

Qualitative analysis of live and dead cells in PLA/TiO_2–OA and PLA/TiO_2 nanocomposites

The results of quantitative MTT and LDH assays were confirmed also by fluorescent staining and confocal microscopy, using LiveDead assay (Fig. 11). Additionally, this method allowed the observation of cell morphology and distribution in contact with PLA nanocomposite scaffolds. After 3 days of culture, a high number of living green cells were observed in contact with PLA–TiO_2–OA-5, whereas the situation found for PLA–TiO_2–OA-10 revealed an equilibrated ratio between live (green) and dead (red) cells. After 7 days of culture, there is a clear difference in the number of cells on the composites, as compared to the pure PLA control, suggesting that the addition of TiO_2 nanoparticles to a certain proportion, as well as nanoparticles functionalization with OA, brings advantages and better biocompatibility properties for the PLA-based scaffolds. In addition, LiveDead analysis also revealed the possibility of cells to group, particularly on PLA/TiO_2–OA-5 nanocomposite. For better observation of cell distribution, 3D reconstructions were performed for all five composites

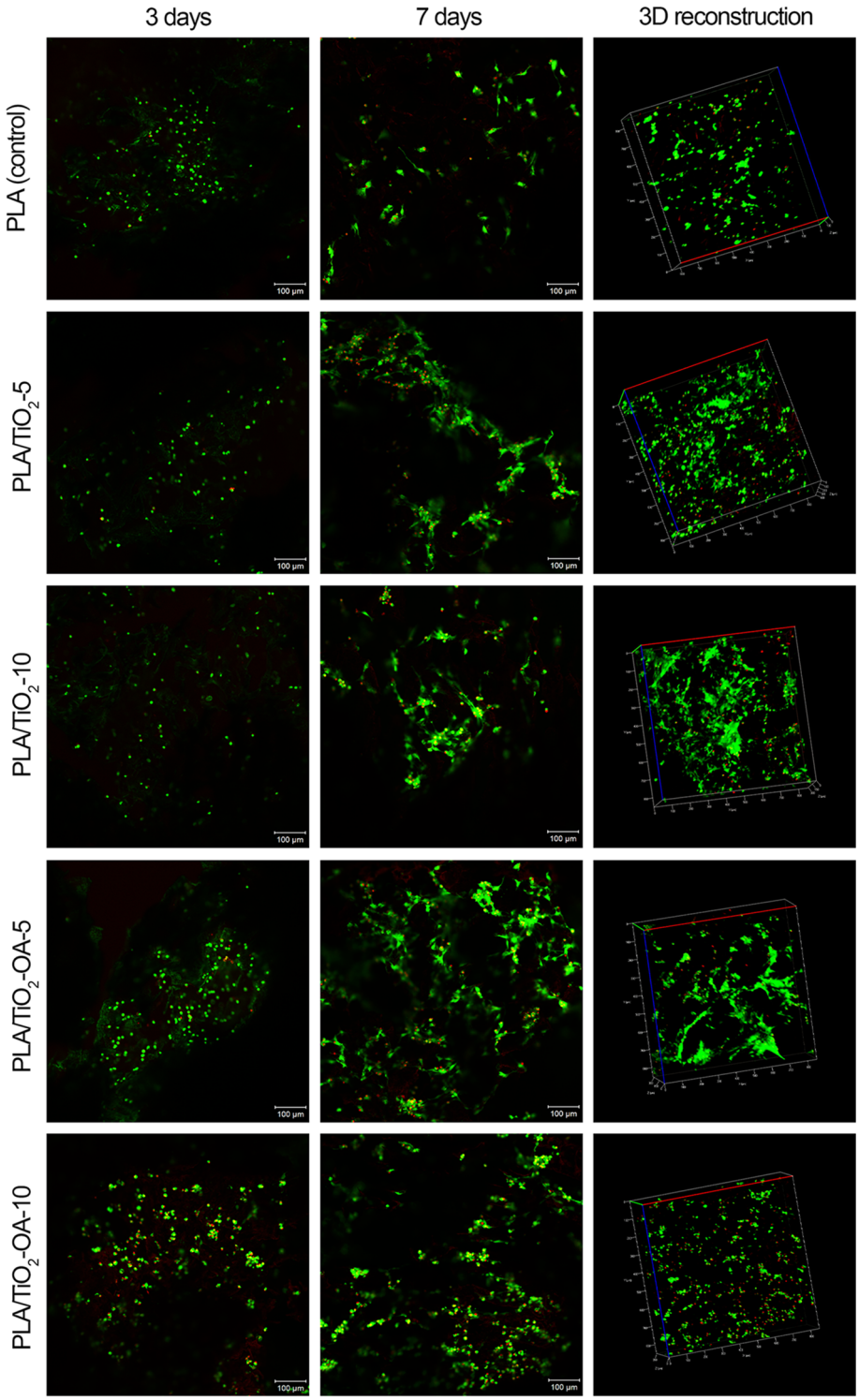

Figure 11 Live (green) and dead (red) cells found in 3D PLA/TiO_2 cultures by LiveDead staining and confocal microscopy; 3D reconstructions showing cell distribution and grouping, as well as the ratio between live and dead cells.

seeded with preosteoblasts (Fig. 10). These reconstructions confirmed the best cell distribution and grouping in PLA/TiO_2–OA-5, suggesting that this composition is the most equilibrated in terms of structural and physicochemical properties among the five studied scaffolds. Both nanocomposite scaffolds filled with unfunctionalized TiO_2 NPs displayed a good biocompatibility, contrarily to PLA–TiO_2–OA-10 scaffold, which showed dispersed non-grouped cells and higher proportion of dead cells.

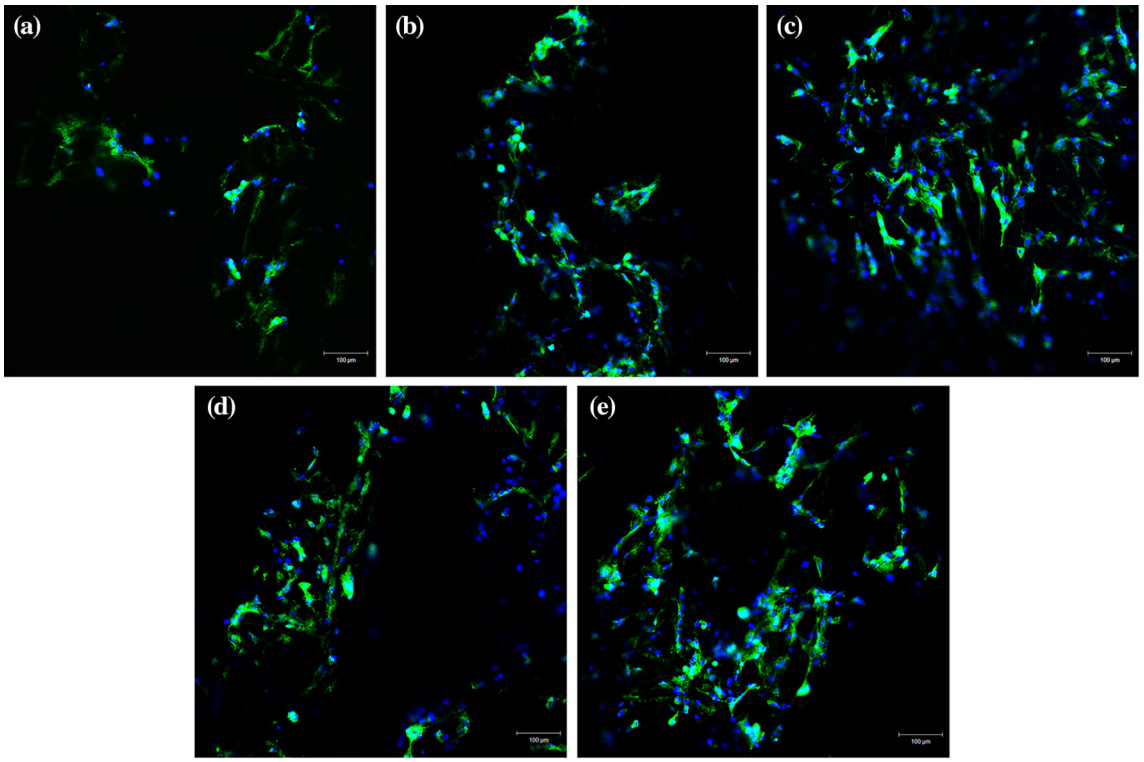

Figure 12 F-Actin fibers developed by preosteoblasts in contact with TiO_2 materials showing cell cytoskeleton and proof of attachment (F-actin- green, cell nuclei- blue). **a** PLA, **b** PLA/TiO_2-5, **c** PLA/TiO_2-10, **d** PLA/TiO_2–OA-5 and **e** PLA/TiO_2–OA-10.

Cytoskeleton development in contact with PLA nanocomposite scaffolds

F-actin filaments were developed by cells in contact with PLA nanocomposites. However, the cells cultivated in contact with PLA displayed grouped actin around the nuclei and not very long actin filaments, suggesting a lower cytoskeletal development in contact with PLA. When adding TiO_2 nanoparticles (5–10%), cells tend to develop longer actin filaments, and in the case of functionalized TiO_2 NPs, cells have developed the best represented cytoskeleton, showing a good biocompatibility of the composites (Fig. 12).

Conclusions

TiO_2 nanoparticles were functionalized with oleic acid (TiO_2–OA) and were used as nanofiller in poly(L-lactic acid) nanocomposite scaffolds. The FTIR data of the modified NPs revealed capping of oleic acid via bidentate chelating interaction.

PLA nanoscaffolds filled with TiO_2–OA nanoparticles were prepared by thermally induced phase separation method. The effect of functionalization nanoparticles was studied in terms of biodegradability, bioactivity and cytocompatibility of the prepared scaffolds, and their potential use as drug delivery systems.

It was shown that PLA/TiO_2–OA nanocomposites possess bioactivity inducing hydroxyapatite when treated in supersaturated fluids. Restricted biodegradation in SBF was identified in investigated nanocomposites when compared to biodegradation of PLA scaffold.

The PLA/TiO_2–OA-5 nanocomposite appeared to be the most biocompatible in terms of cell viability and proliferation, as compared to pure PLA and composites prepared with the same content of unfunctionalized nanofiller.

Insignificant cell proliferation and increased cytotoxicity were identified in the nanocomposite with 10 wt% of TiO_2–OA nanofiller.

Acknowledgements

The authors of the paper would like to thank Dr. Chiara Gualandi (Department of Chemistry "G.

Ciamician", University of Bologna) for her help with the SEM measurements.

References

[1] Armentano I, Dottori M, Fortunati E, Mattioli S, Kenny JM (2010) Biodegradable polymer matrix nanocomposite for tissue engineering: a review. Polym Degrad Stabil 95:2126–2146

[2] Armentano I, Bitinis N, Fortunati E, Mattioli S, Rescignano N, Verdejo R, Lopez-Manchado MA, Kenny JM (2013) Multifunctional nanostructured PLA materials for packaging and tissue engineering. Prog Polym Sci 38:1720–1747

[3] Pellis A, Silvestrini L, Scaini D, Coburn JM, Gardossi L, Kaplan DL, Acero EH, Guebitz GM (2017) Enzyme-catalyzed functionalization of poly(L-lactic acid) for drug delivery applications. Process Biochem Part A 59:77–83

[4] Dorati R, De Trizio A, Modena T, Conti B, Benazzo F, Gastaldi G, Genta I (2017) Biodegradable scaffolds for bone regeneration combined with drug-delivery systems in osteomyelitis therapy. Pharmaceuticals 96:10–21

[5] Davachi SM, Kaffashi B (2015) Polylactic acid in medicine. Polym Plast Technol Eng 54:944–967

[6] Ruiz-Hitzky E, Fernandes FM (2013) Progress in bio-nanocomposites: from green plastics to biomedical applications. Prog Polym Sci 38:1389–1772

[7] Allo BA, Costa DO, Dixon SJ, Mequanint K, Rizkalla A (2012) Bioactive and biodegradable nanocomposites and hybrid biomaterials for bone regeneration. J Funct Biomater 3:432–463

[8] Goreham RV, Mierczyska A, Smith LE, Sedev R, Vasilev K (2013) Small surface nanotopography encourages fibroblast and osteoblast cell adhesion. RCS Adv 3:10309–10317

[9] Lin ASP, Barrows TH, Cartmell SH, Guldberg RE (2003) Microarchitectural and mechanical characterization of oriented porous polymer scaffolds. Biomaterials 24:481–489

[10] Wilberforce SIJ, Finlayson CE, Best SM, Cameron R (2011) A comparative study of the thermal and dynamic mechanical behaviour of quenched and annealed poly-L-lactide/α-tricalciumphosphate nanocomposites. Acta Biomater 7:2176–2184

[11] Kim SS, Park MS, Jeon O, Choi CY, Kim BS (2006) Poly(lactide-co-glucolide)/hydroxyapatite composite scaffolds for bone tissue engineering. Biomaterials 27:1399–1409

[12] Mantsos T, Chatzistavrou X, Roether JA, Hupa L, Arstila H, Boccaccini AR (2009) Non-crystalline composite tissue engineering scaffolds using boron containing bioactive glass and poly(D, L-lactic acid) coatings. Biomed Mater 4:055002. https://doi.org/10.1088/1748-6041/4/5/055002

[13] Armentano I, Marinucci L, Dottori M, Balloni S, Fortunati E, Penacchi M, Becchetti E, Locci P, Kenny JM (2011) Novel poly(L-lactide) (PLLA)/SWCNTs nanocomposites for biomedical application: material characterization and biocompatibility evaluation. J Biomat Sci Polym E 22:541–556

[14] Bocccaccini A, Blaker J, Maquet V, Chung W, Jerome R, Nazhat S (2006) Poly(D, L-lactide) (PDLLA) foams with TiO2 nanoparticles and (PDLLA)/TiO2-Bioglass foam composites for tissue engineering scaffolds. J Mater Sci 41:3999–4008. https://doi.org/10.1007/s10853-006-7575-7

[15] Wei J, Chen QZ, Stevens MM, Roether JA, Boccaccini AR (2008) Biocompatibility and bioactivity of PDLLA/TiO_2 and PDLLA/TiO_2/Bioglass nanocomposites. Mater Sci Eng, C 28:1–10

[16] Uchida M, Kim HM, Kokubo T, Fujibayashi S, Nakamura T (2003) Structural dependence of apatite formation on titania gels in a simulated body fluid. J Biomed Mater Res A 64:164–170

[17] Oberdörter G (2000) Pulmonary effects of inhaled ultrafine particles. Int Arch Occup Environ Health 74:1–8

[18] Bhattacharya K, Davoren M, Boertz J, Schins RPF, Hoffmann E, Dopp E (2009) Titanium dioxide nanoparticles induce oxidative stress and DNA-adduct formation but not DNA-breakage in human lung cells. Part Fibre Toxicol 6:17. https://doi.org/10.1186/1743-8977-6-17

[19] Petkovic J (2011) DNA damage and alterations in expression of DNA damage responsive genes induced by TiO_2 nanoparticles in human hepatoma HepG2cells. Nanotechnology 5:341–353

[20] Treccani L, Klein TY, Meder F, Pardun K, Rezwan K (2013) Functionalized ceramics for biomedical and environmental applications. Acta Biomater 9:7115–7150

[21] Xie J, Pan X, Wang M, Ma J, Fei Y, Wang PN, Mi L (2016) The role of surface modification for TiO_2 nanoparticles in cancer cells. Colloids Surf B 143:148–155

[22] Fisher EW, Sterzel HJ, Wegner G (1973) Investigation of the structure of solution grown crystals of lactide copolymers by means of chemical. Coll Polym Sci 251:980–990

[23] Ma PX, Zhang RJ (1999) Synthetic nano-scale fibrous extracellular matrix. J Biomed Res 46:60–72

[24] Kokubo T, Kushitani H, Sakka S, Kitsugi T, Yamamuro T (1990) Solutions able to produce in vivo surface-structure changes in bioactive glass-ceramic A-W. J Biomed Mater Res A 24:721–734

[25] Bracci B, Panzavolta S, Bigi A (2013) A new simplified calcifying solution to synthesize calcium phosphate coatings. Surf Coat Technol 232:13–21

[26] Silvetrein PM, Webster FX (1997) Spectrometric identification of organic compounds, 6th edn. Wiley, New York
[27] Dobson KD, McQuillian AJ (2000) Insitu infrared spectroscopic analysis of the adsorption of aromatic carboxylic acids to TiO_2, Zr, O_2, Al_2O_3 and Ta_2O_5 from aqueous solutions. Spectrochim Acta A 56:557–565
[28] Shete PB, Patil RM, Tiwale BM, Pawar SH (2015) Water dispersible oleic acid-coated Fe_3O_4 nanoparticles for biomedical application. J Magn Magn Mater 377:406–410
[29] Auras R, Lim LT, Susan E, Selke M, Tsuji H (2010) Poly (lactic acid): synthesis, structures, properties, processing, and application. Wiley, New Jersey
[30] Blomergen S, Holden D, Hamer G, Bluhm T, Marchessault R (1986) Studies of composition and crystallinity of bacterial poly(β-hydroxybutyrate-co-β-hydroxyvalerate). Macromolecules 19:2865–2871
[31] Buzarovska A, Gozdanov A (2012) Bidegradable Poly(L-lactic acid)/TiO_2 nanocomposites: thermal properties and degradation. J Appl Polym Sci 123:2187–2193
[32] Buzarovska A, Qualandi C, Parrilli A, Scandola M (2015) Effect of TiO_2 nanoparticle loading on Poly(L-lactic acid) porous scaffolds fabricated by TIPS. Compos Part B Eng 81:189–195
[33] Mandelkern L (2004) Crystallization of polymers: kinetics and mechanisms, vol 2, 2nd edn. Cambridge University Press, Cambridge
[34] Haugh MG, Murphy CM, O'Brien FJ (2010) Novel freeze-drying methods to produce a range of collagen–glucosaminoglucan scaffolds with tailored mean pore size. Tissue Eng Part C 16:887–894
[35] Leung LH, Chan C, Baek S, Naguib H (2008) Comparison of morphology and mechanical properties of PLGA bioscaffolds. Biomed Mater 3(2):025006. https://doi.org/10.1088/1748-6041/3/2/025006
[36] Leung LH, Perron J, Naguib HE (2007) A study of the mechanics of porous PLGA 85/15 scaffold in compression. Polym Polym Compos 15(6):437–443
[37] Kong L, Gao Y, Lu G, Gong Y, Zhao N, Zhang X (2006) A study of bioactivity of chitosan/nano-hydroxyapatite composite scaffolds for bone tissue engineering. Eur Polym J 42:3171–3179
[38] Zhang J, Yin HM, Hsiao BS, Zhong GJ, Li ZM (2014) Biodegradable poly(lactic acid)/hydroxyl apatite 3D porous scaffolds using high-pressure molding and salt leaching. J Mater Sci 49:1648–1658. https://doi.org/10.1007/s10853-013-7848-x
[39] Prabaharan M, Rodriguez-Perez MA, deSaja JA, Mano JE (2007) Preparation and Characterization of Poly(L-lactic acid)-chitosan hybrid scaffolds with drug release capability. J Biomed Mater Res B 81:427–434
[40] Guo Z, Yang C, Zhou Z, Chen S, Li F (2017) Characterization of biodegradable poly(lactic acid) porous scaffolds prepared using selective enzymatic degradation for tissue engineering. RSC Adv 7:34063–34070
[41] Ha CS, Cho W (2002) Miscibility, properties, and biodegradability of microbial polyester containing blends. J Prog Polym Sci 27:759–809
[42] He Y, Inoue Y (2000) Novel FTIR method for determining the crystallinity of poly(ε-caprolactone). Polym Int 49:623–626
[43] Fonseca C, Ochoa A, Ulloa MT, Alvarez E, Canales D, Zapata PA (2015) Poly(lactic acid)/TiO_2 nanocomposites as alternative biocidal and antifungal materials. Mater Sci Eng, C 57:314–320
[44] Costa P (2015) Bone tissue engineering drug delivery. Curr Mol Bio Rep 1:87–93
[45] Dash TK, Konkimalla B (2012) Poly-caprolactone based formulations for drug delivery and tissue engineering. J Control Release 158:15–33
[46] Kayal S, Ramanujan RV (2010) Doxorubicin loaded PVA coated iron oxide nanoparticles for targeted drug delivery. Mater Sci Eng, C 30:484–490
[47] Illie A, Ghitulica C, Andronescu E, Cucuruz A, Fiscai A (2016) New composite materials on alginate and hydroxyapatite as potential carriers for ascorbic acid. Int J Pharm 510:501–507
[48] Hue J, Prabhakaran MP, Tian L, Ding X, Ramakrishna S (2015) Drug-loaded emulsion electrospun nanofibers: characterization, drug release and invitro biocompatibility. RSC Adv 5:100256–100267
[49] Pereira R, Bartolo PJ (2013) Degradation behavior of biopolymer-based membranes for skin tissue engineering. Procedia Eng 59:285–291